New Journal of Physics
The open access journal at the forefront of physics

Deutsche Physikalische Gesellschaft DPG
IOP Institute of Physics

PAPER • OPEN ACCESS

Coherence turned on by incoherent light

To cite this article: Vyacheslav N Shatokhin *et al* 2018 *New J. Phys.* **20** 113040

View the article online for updates and enhancements.

IOP ebooks™

Bringing you innovative digital publishing with leading voices to create your essential collection of books in STEM research.

Start exploring the collection - download the first chapter of every title for free.

This content was downloaded from IP address 163.1.203.194 on 29/11/2018 at 11:25

IOP Publishing New J. Phys. **20** (2018) 113040 https://doi.org/10.1088/1367-2630/aaf08f

New Journal of Physics
The open access journal at the forefront of physics

Deutsche Physikalische Gesellschaft DPG
IOP Institute of Physics

Published in partnership with: Deutsche Physikalische Gesellschaft and the Institute of Physics

OPEN ACCESS

RECEIVED
7 August 2018

REVISED
5 November 2018

ACCEPTED FOR PUBLICATION
13 November 2018

PUBLISHED
28 November 2018

Original content from this work may be used under the terms of the Creative Commons Attribution 3.0 licence.

Any further distribution of this work must maintain attribution to the author(s) and the title of the work, journal citation and DOI.

PAPER

Coherence turned on by incoherent light

Vyacheslav N Shatokhin[1], **Mattia Walschaers**[1,2,3], **Frank Schlawin**[1,4] **and Andreas Buchleitner**[1]

[1] Physikalisches Institut, Albert-Ludwigs-Universität Freiburg, Hermann-Herder-Str. 3, D-79104 Freiburg, Germany
[2] Instituut voor Theoretische Fysica, KU Leuven, Celestijnenlaan 200D, B-3001 Heverlee, Belgium
[3] Laboratoire Kastler Brossel, UPMC-Sorbonne Universités, CNRS, ENS-PSL Research University, Collège de France; 4 place Jussieu, F-75252 Paris, France
[4] Clarendon Laboratory, University of Oxford, Parks Road, Oxford OX1 3PU, United Kingdom

E-mail: vyacheslav.shatokhin@physik.uni-freiburg.de

Keywords: molecular aggregate, dipole–dipole interaction, thermal photons, energy transfer, coherence

Abstract

One of the most pertinent problems in the debate on non-trivial quantum effects in biology concerns natural photosynthesis. Since sunlight is composed of thermal photons, it was argued to be unable to induce quantum coherence in matter, and that quantum mechanics is therefore irrelevant for the dynamical processes following photoabsorption. Our present analysis of a toy 'molecular aggregate'—composed of two dipole–dipole interacting two-level atoms treated as an open quantum system—however shows that incoherent excitations indeed can trigger persistent, coherent dynamics in both the site and the exciton bases: we demonstrate that collective decay processes induced by the dipole–dipole interactions create coherent intermolecular transport—regardless of the coherence properties of the incoming radiation. Our analysis shows that the steady state coherence is mediated by the population imbalance between the molecules and, therefore, *increases* with the energy difference between the two-level atoms. Our results establish the importance of collective decay processes in the study of ultrafast photophysics, and especially their potential role to generate stationary coherence in incoherently driven quantum transport.

1. Introduction

A detailed understanding of the microscopic processes which underlie natural photosynthesis represents an important and intriguing source of inspiration for technologies which seek to efficiently capture, transform, and store solar energy [1, 2]. One of the most important open questions in this research area is whether quantum interference effects play a role in solar light harvesting, and possibly could be used for highly efficient solar energy conversion [3, 4]. That transient quantum coherence can prevail in such complex structures, at ambient temperatures, has been suggested based on experimental data [3, 5, 6], and has also been reported for the charge separation process in organic solar cells [7, 8].

It however is argued [9] that the evidence provided by the above experiments is inconclusive, because the conditions under which quantum effects were experimentally observed in certain light harvesting complexes (LHC) differ from conditions *in vivo*. Indeed, laboratory experiments rely on photon echo spectroscopy [10], where the energy transfer is induced by a series of ultrashort coherent laser pulses. In contrast, sunlight (driving the natural process) can be described as continuous wave (or stationary) thermal (incoherent) radiation [11]. Thus, it is *a priori* crucial to distinguish the coherence observed in photon echoes [12] from coherence which may arise in non-equilibrium open system quantum dynamics—as we will outline below.

Moreover, some models [9, 13, 14] suggest that the coupling of a quantum system to a thermal radiation bath rapidly leads to the formation of a stationary state that does not exhibit any coherences. This apparently contradicts the point of view that coherent non-equilibrium transport processes—leading to the observed efficiency of the excitation transfer [15–17]—can be triggered by any photoabsorption event [18], regardless of the source of photons.

Here we develop a microscopic quantum optical theory to resolve this longstanding controversy. Specifically, we establish that steady state coherence can indeed emerge in an incoherently driven molecular

© 2018 The Author(s). Published by IOP Publishing Ltd on behalf of Deutsche Physikalische Gesellschaft

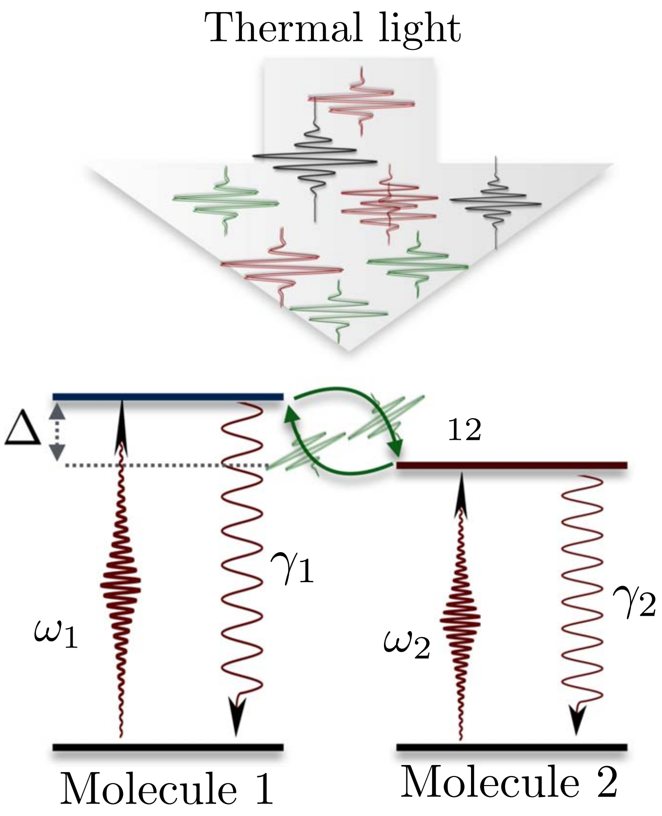

Figure 1. Two molecules at a distance r_{12} and with transition frequencies ω_1 and ω_2, detuned by $\Delta = \omega_1 - \omega_2$, are embedded into a common electromagnetic bath. The bath induces radiative decay of the molecules (γ_k is the decay rate of molecule k), as well as a dipole–dipole interaction with complex coupling constant T_{12} (see (2)). An external, incoherent thermal source stimulates absorption and emission processes.

complex, under realistic assumptions on the incident wave lengths and molecular separations. To begin with, we recall that the primary process of photosynthesis is the absorption of a single photon by a chlorophyll molecule, whereby the molecule undergoes a transition from the ground to the excited electronic state [2]. The photoabsorption initiates energy transfer towards the reaction center, where a charge separation cascade with almost unit efficiency is triggered [19]. This transfer process from the initial absorption event to the charge separation has a finite duration, of the order of 10–100 ps [20], and it is during this process that transient electronic coherences have been observed [5, 6, 20, 21]. Afterwards, the molecule resets in its ground electronic state and is able to absorb the next photon. We will show that, when averaging over many such single photon absorption and transfer cycles, one ends up with a master equation-type ensemble description which exhibits non-vanishing coherence in the non-equilibrium steady state.

Inspired by light-harvesting systems, we consider a 'molecular aggregate' which consists of two effective two-level atoms [22]—which we shall refer to as molecules in the following—that are embedded into a common electromagnetic bath. Thereby, we abstract ourselves from the details of the structure and energy spectra of a real photosynthetic complex [2]. Nonetheless, our dimer model is able to describe two absorption bands associated with the widths of the electronic excited states, as well as the dipole–dipole interaction between the molecules. We study the interaction of this system with an external incoherent field which represents the sunlight, and show that coherent evolution survives even in the non-equilibrium *steady* state of the incoherently driven system, as a reflection of the transient coherences induced on the level of single photon absorption and transport processes.

2. Model

Our model is presented in figure 1. It consists of two molecules embedded, at a distance r_{12}, into a common radiation bath and interacting with an external incoherent radiation field in the optical frequency range. We assume that the molecules have allowed dipole transitions between their electronic ground and excited states $|g_k\rangle$ and $|e_k\rangle$, $k = 1, 2$, respectively, and that their optical transition frequencies ω_1 and ω_2 are detuned with $\Delta = \omega_1 - \omega_2 \ll \omega_1, \omega_2$. Furthermore, we can ignore the ambient thermal photons at optical frequencies and therefore assume the relevant modes of the radiation reservoir in the vacuum state. This bath induces spontaneous decay of the individual molecules with rates γ_k, as well as their dipole–dipole interaction with complex coupling strength T_{12}. Additionally, the coupling to other, e.g. vibrational, degrees of freedom may cause further dissipation [15, 23], which is not considered in this work. As for the external incoherent field, we assume that its energy density is a slowly varying function around the transition frequency. The external field generates absorption and stimulated emission processes at the rate $\gamma_k N(\omega_k)$ [24], where $N(\omega_k)$ is the average number of the (incoherent) source photons at the transition frequency, which is defined by the source temperature. The linearity of the light-matter coupling ensures that, as long as optical nonlinearities are weak (this is the case, since the mean number of the incident photons ≈0.01, see below), the dipolar interaction between the two atoms is not affected by the presence of an external light field.

Using standard quantum optical methods [25, 26], one can trace out the bath degrees of freedom, to arrive at the master equation governing the evolution of the 'aggregate' density matrix ρ, in the (site) basis of the uncoupled individual molecules' energy eigenstates $\{|g_1, g_2\rangle, |e_1, g_2\rangle, |g_1, e_2\rangle, |e_1, e_2\rangle\}$. In the frame rotating at the average frequency $\omega_0 = (\omega_1 + \omega_2)/2$ wherein rapidly oscillating terms are eliminated since $\omega_1 \approx \omega_2$, the master equation reads

$$\dot{\varrho} = \sum_{k\neq l=1}^{2}\left(\frac{\mathrm{i}\Delta}{2}(-1)^k[\sigma_+^k\sigma_-^k, \varrho] - \mathrm{i}\Omega[\sigma_+^k\sigma_-^l, \varrho] + \gamma_k N(\omega_k)\{[\sigma_+^k, \varrho\sigma_-^k] + [\sigma_+^k\varrho, \sigma_-^k]\}\right.$$
$$\left. + \gamma_k\{1 + N(\omega_k)\}\{[\sigma_-^k, \varrho\sigma_+^k] + [\sigma_-^k\varrho, \sigma_+^k]\} + \Gamma\{[\sigma_-^k, \varrho\sigma_+^l] + [\sigma_-^k\varrho, \sigma_+^l]\}\right). \tag{1}$$

In this equation, the atomic (de-)excitation operators are given as $\sigma_-^k = |g_k\rangle\langle e_k|$, $\sigma_+^k = |e_k\rangle\langle g_k|$, the atomic decay rates read $\gamma_k = d_k^2\omega_k^3/6\pi\epsilon_0\hbar c^3$, and $\Gamma \equiv \Gamma(\omega_0 r_{12}/c)$, $\Omega \equiv \Omega(\omega_0 r_{12}/c)$ are the real and imaginary parts, respectively, of the *retarded* dipole–dipole interaction strength $T_{12} = \Gamma + \mathrm{i}\Omega$, which in particular generates collective effects such as super-radiance [26–28][5]. The physical meaning of the real and imaginary parts of T_{12} can be unambiguously identified from the structure of the master equation (1): terms proportional to $\mathrm{i}\Omega$ describe oscillatory, reversible, non-radiative excitation exchange between both molecules, and lead to the formation of delocalized excitonic states. Terms proportional to Γ represent (collective) radiative decay processes, following a non-radiative excitation exchange between the molecules. Accordingly, Γ and Ω are associated with the life time and the energy shift of the (entangled, Dicke) eigenstates $|\psi_+\rangle$, $|\psi_-\rangle$ (see appendix A) of the dipole-coupled molecular dimer, respectively [26, 30, 31]. Explicitly, Γ and Ω are given as [26, 27, 32],

$$\Gamma(\xi) \equiv \frac{3\sqrt{\gamma_1\gamma_2}}{2}\left\{[\hat{\mathbf{d}}_1\cdot\hat{\mathbf{d}}_2 - (\hat{\mathbf{d}}_1\cdot\hat{\mathbf{r}}_{12})(\hat{\mathbf{d}}_2\cdot\hat{\mathbf{r}}_{12})]\frac{\sin\xi}{\xi} + [\hat{\mathbf{d}}_1\cdot\hat{\mathbf{d}}_2 - 3(\hat{\mathbf{d}}_1\cdot\hat{\mathbf{r}}_{12})(\hat{\mathbf{d}}_2\cdot\hat{\mathbf{r}}_{12})]\right.$$
$$\left.\times\left(\frac{\cos\xi}{\xi^2} - \frac{\sin\xi}{\xi^3}\right)\right\}, \tag{2a}$$

$$\Omega(\xi) \equiv \frac{3\sqrt{\gamma_1\gamma_2}}{2}\left\{-[\hat{\mathbf{d}}_1\cdot\hat{\mathbf{d}}_2 - (\hat{\mathbf{d}}_1\cdot\hat{\mathbf{r}}_{12})(\hat{\mathbf{d}}_2\cdot\hat{\mathbf{r}}_{12})]\frac{\cos\xi}{\xi} + [\hat{\mathbf{d}}_1\cdot\hat{\mathbf{d}}_2 - 3(\hat{\mathbf{d}}_1\cdot\hat{\mathbf{r}}_{12})(\hat{\mathbf{d}}_2\cdot\hat{\mathbf{r}}_{12})]\right.$$
$$\left.\times\left(\frac{\sin\xi}{\xi^2} + \frac{\cos\xi}{\xi^3}\right)\right\}, \tag{2b}$$

where $\xi \equiv \omega_0 r_{12}/c$ is the effective intermolecular distance[6], and $\hat{\mathbf{d}}_k$ and $\hat{\mathbf{r}}_{12}$ are unit vectors directed along the kth molecular dipole and along the vector connecting the molecules, respectively. Note that the far-field terms in (2a), (2b) (i.e. the terms decreasing as ξ^{-1} for $\xi \gg 1$) describe retardation effects proper that are associated with the exchange of real photons [27]. These effects start playing a role at $r_{12} \gtrsim 10$ nm [29], though they are deemed unimportant at inter-molecular distances of less than 10nm (i.e. $\xi \lesssim 0.1$).

One of the key processes in the theory of photosynthesis is resonance energy transfer [22]. This transfer is effective between molecules whose transition frequencies are close to each other (hence, the name of the process) and is characterized by a rate proportional to $|\Gamma + \mathrm{i}\Omega|^2$ [27]. In the non-retarded limit $\xi \ll 1$, $\Gamma(\xi)$ is much smaller than $\Omega(\xi)$. It is therefore common practice to neglect $\Gamma(\xi)$, and to retain only the non-retarded contributions of $\Omega(\xi)$ [22, 34, 35]. In this limit, $\Omega(\xi) \to V_{\mathrm{dd}}/\hbar$, with V_{dd} the static dipole–dipole interaction energy [26, 28]:

$$V_{\mathrm{dd}} = \frac{\mathbf{d}_1\cdot\mathbf{d}_2 - 3(\mathbf{d}_1\cdot\hat{\mathbf{r}}_{12})(\mathbf{d}_2\cdot\hat{\mathbf{r}}_{12})}{4\pi\epsilon_0 r_{12}^3}. \tag{3}$$

---

[5] In the chemical physics literature [27–29], the complex retarded dipole–dipole interaction strength is defined as $\Omega + \mathrm{i}\Gamma$, which up to a phase factor coincides with the one adopted in this work.

[6] For optical wave lengths of 400–900 nm, and for typical distances r_{12} between the chlorophyll molecules in different LHCs varying from 1 to 10 nm [2, 33], effective distances lie in the range $\xi \sim 0.01$–0.1.

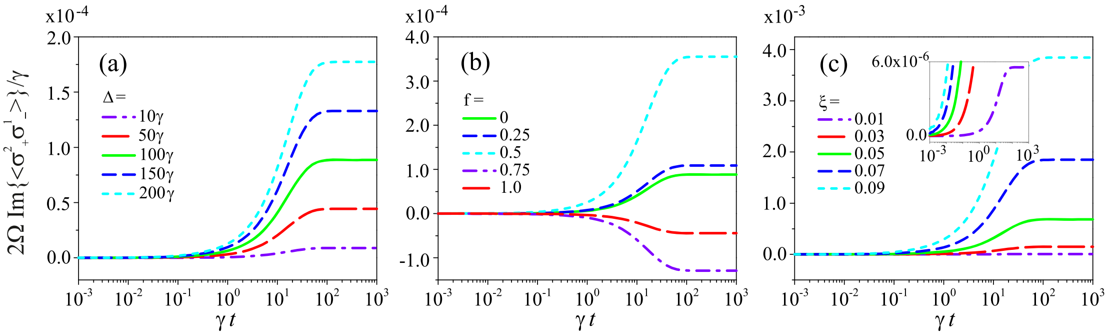

Figure 2. The inter-molecular electronic-coherence-induced excitation current $2\Omega\,\mathrm{Im}\{\langle\sigma_+^2(t)\sigma_-^1(t)\rangle\}$, as generated by (1) (on a semi-log scale), with $N(\omega_1) = N(\omega_2) = N(\omega_0) = 0.01$ (corresponding to a source temperature $T \approx 6000$ K), for realistic choices of the characteristic parameters (see legends) which define the molecular dimer's dynamics: (a) variation of the molecular detuning Δ, at $\xi = 0.02$ (or $r_{12} = 1.5$ nm), $\mathrm{f} = 0$. (b) Variable dipole orientation f, at $\xi = 0.02$, $\Delta = 100\gamma$. (c) Variable distance ξ (the values 0.01, 0.03, 0.05, 0.07, 0.09 correspond to $r_{12} = 0.73, 2.2, 3.7, 5.1, 6.6$ nm, respectively) of the dimer's constituent molecules, at $\mathrm{f} = 0$, $\Delta = 50\gamma$.

This wide-spread approximation however neglects that also $\Gamma(\xi)$ does remain finite as $r_{12} \to 0$, with $\Gamma(\xi) \to \sqrt{\gamma_1\gamma_2}\,\hat{\mathbf{d}}_1 \cdot \hat{\mathbf{d}}_2$, and (3) is thus imprecise at small distances. As we show below, a consequence of using the approximate expression (3) is that a collective coherent effect—the stationary excitation current in the dipole-interacting system—is erroneously predicted to vanish.

Let us inspect the time-dependent expectation value $\mathrm{Im}\,\{\langle\sigma_+^2(t)\sigma_-^1(t)\rangle\} \equiv \mathrm{Im}\,\{\langle e_1, g_2|\varrho(t)|g_1, e_2\rangle\} \equiv \mathrm{sign}(\Omega)\,\mathrm{Im}\,\{\langle\psi_+|\varrho(t)|\psi_-\rangle\}$ (see appendix A) as the quantifier of, respectively, the inter-site and excitonic coherence of our 'molecular aggregate' under incoherent driving. It should be stressed that the magnitude of the current is the same in the site and the exciton bases—the two natural physical bases for the dimer. In this respect, our measure of coherence can be regarded as basis independent. However, motivated by excitation transport, we prefer to study coherence in the site basis. Upon multiplication by 2Ω this yields the *excitation current*, which is proportional to the probability per unit time for an excitation transfer from molecule 1 to molecule 2 (see appendix B). For simplicity and without loss of essential physics, we study the temporal behavior of this coherence-induced current under the assumptions that the thermal source is characterized by $N(\omega_0) = 0.01$ (which is consistent with the mean photon number of the sunlight at the optical frequencies), both dipoles point in the same direction, and that the excited states of molecules 1 and 2 have equal linewidths $\gamma_1 = \gamma_2 = \gamma$[7]. Furthermore, we assume that $\Delta > 0$, by noting that in a fully symmetric system, where $\gamma_1 = \gamma_2$ and $\Delta = 0$, the expectation value of the excitation current trivially vanishes for all times, i.e. $\mathrm{Im}\,\{\langle\sigma_+^2(t)\sigma_-^1(t)\rangle\} \equiv 0$, while the treatment of the case $\Delta < 0$ amounts to relabeling molecules 1 and 2.

Our results on the temporal evolution of $2\Omega\,\mathrm{Im}\,\{\langle\sigma_+^2(t)\sigma_-^1(t)\rangle\}$ are plotted in figures 2(a)–(c), where we vary the detuning Δ, the orientation $\mathrm{f} = (\hat{\mathbf{d}}_1 \cdot \hat{\mathbf{r}}_{12})$, or the effective distance ξ, respectively, while keeping the two remaining parameters fixed. It is evident that a non-vanishing current is a generic feature of the intramolecular excitation transfer that follows the photo-absorption process by the molecular aggregate prepared in its ground (reset) state at $t = 0$. The non-equilibrium coherence emerges on time scales $t \gtrsim 10^{-3}\gamma^{-1}$, when radiative relaxation processes come into play. At $t \gg \gamma^{-1}$, the excitation current tends to its steady state value mono-exponentially

$$2\Omega\,\mathrm{Im}\,\{\langle\sigma_+^2(t)\sigma_-^1(t)\rangle\} = \frac{4N(\omega_0)\Omega\Gamma[1 + 2N(\omega_0)]\gamma^2\Delta}{R}\{1 - \exp(-Ct)\}, \tag{4}$$

where $C \equiv C(\xi,\ \mathrm{f},\ \Delta) \sim \gamma N(\omega_0)$ and R is given in (B.14). This contrasts the dynamics of a V-type three-level system driven by incoherent light, where long-lived coherences exhibit damped oscillations or slow exponential decay [36].

Equation (4) shows that the stationary excitation current *only* emerges for a non-vanishing collective decay rate Γ, giving rise to the irreversibility of the excitation exchange process[8]. As a result, the stationary populations of the excited levels of the two molecules become unequal, which is crucial for the emergence of the stationary current. It is also evident from (4) that the population imbalance and, hence, the current in the steady state

---

[7] This can be justified by using a standard expression for the spontaneous decay rate γ_k (see its definition following (1)). If we assume that both dipoles have equal matrix elements and their transition frequencies lie in the optical domain, then for $\omega_1 = 2\pi \times 10^{15}$ Hz, $\omega_2 = \omega_1 - \Delta$ and $\Delta = 10$ GHz (which corresponds to $\simeq$100 natural linewidths), we obtain, $\gamma_2/\gamma_1 \approx 1 - 3\Delta/\omega_1 = 0.99997$.

[8] Finite steady state electronic coherence may arise for vanishing Γ if one allows for the coupling of the electronic excitations to additional degrees of freedom, as discussed in [35].

increase with Δ. On the other hand, the current decreases as Ω increases (that is, as ξ decreases, see figure 2(c)). A qualitatively similar dependence of stationary coherence on Ω was predicted in a more realistic photosynthetic dimer model including incoherent pumping, phonon-induced relaxation, dephasing, and trapping even in the absence of collective decay processes [37]. More explicitly, the stationary coherence and the population imbalance are in fact proportional to one another (see appendix B):

$$2\Omega\ \mathrm{Im}\ \{\langle\sigma_+^2\sigma_-^1\rangle\} = \frac{\kappa}{2}\{\langle\sigma_+^2\sigma_-^2\rangle - \langle\sigma_+^1\sigma_-^1\rangle\}. \tag{5}$$

Here, $\kappa = 2\gamma(1 + 2N)$ and $\langle\sigma_+^k\sigma_-^k\rangle = \langle e_k|\varrho^k|e_k\rangle$, with $\varrho^k = \mathrm{Tr}_l(\varrho)$ $(k,\ l = 1,\ 2,\ k \neq l)$ the reduced density matrix of molecule k. This result can be interpreted as an energy balance relation for our dipole–dipole coupled system: the left-hand side of (5) yields the number of photons that is transferred per unit time from molecule 1 to molecule 2; the right-hand side yields the difference between the total number of photons that are emitted, or absorbed, per unit time, by molecule 2 and 1, due to spontaneous and stimulated emission.

Equation (5) is reminiscent of relations well known in single atom resonance fluorescence [38, 39]: there, quantum coherence between the atomic ground and excited states arises due to the presence of the laser field, characterized by the Rabi frequency. The quantity describing the atomic coherence, $\mathrm{Im}\ \{\langle\sigma_+\rangle\}$, is coupled to the atomic excited state population, such that single atom energy balance relations similar to (5) hold. In our present case of two molecules, quantum coherence between the molecular dipoles arises due to the dipole–dipole interaction, playing the role of the Rabi frequency. The directed excitation current leads to an imbalance of the molecular excited state populations: the molecule with larger transition frequency $\omega_1 > \omega_2$ has smaller excited state population because part of it is coherently transferred to the molecule with smaller transition frequency ω_2. The magnitude of the current is highly sensitive to the dimer's parameters and is typically $\simeq 10^2$–10^4 excitation transfer events per second (see figure 2), or about 0.01%–1% of the incoherent pumping rate $\gamma N(\omega_0) \simeq 10^6\ \mathrm{s}^{-1}$, assuming $\gamma \simeq 10^8\ \mathrm{s}^{-1}$.

The above scenario of the downhill excitation current is apparently violated for the orientations f for which Ω is negative (see, e.g. the dashed–dotted and long dashed lines in figure 2(b)). Yet, in the dimer's eigenbasis the stationary current always flows towards the state with smaller energy (see appendix A).

3. Unraveled dynamics

At first glance, the monotonic build-up of the stationary current in figure 2 may seem inconsistent with the transient character of the observed quantum coherences [5, 6]. However, the typical behavior of the current can be viewed as a result of an average over an ensemble of 'quantum trajectories' [40, 41] (see figure 3(a)) corresponding to individual incidents of an excitation process in our 'molecular aggregate' (see appendix C): Initially (re-)set in their ground state, molecule 1 or 2 absorbs a photon (undergoes a 'quantum jump' mediated by the operator σ_+^1 or σ_+^2), with relative probability one half, at a random moment in time $t_0 > 0$. The photoabsorption prepares the dimer in either the state $|e_1,\ g_2\rangle$ or $|g_1,\ e_2\rangle$ and launches coherent evolution within the single excitation subspace governed by the Hamiltonian H_D (see appendix A). The coherent exchange of the excitation between the molecules generated by the latter Hamiltonian translates into a transient oscillation of the excitation current at frequency $\sqrt{4\Omega^2 + \Delta^2}$, see figure 3(c). If a photon is emitted by the dimer at a random time t_1 such that $t_1 - t_0 < \gamma^{-1}$, then this happens primarily as a result of a quantum jump described by the collective operator $(\sigma_-^1 + \sigma_-^2)$ (see appendix C). The dimer is then reset to its ground state, until the next photon absorption occurs. For some incidents of the excitation process, the photoemission does not occur at times $t_1 - t_0 < \gamma^{-1}$ and the envelope of the current exponentially decreases on a time scale $\sim 10\gamma^{-1}$ (figure 3(b)) to a finite value (see appendix C). This corresponds to the continuous evolution of the dimer into a conditioned state that is close to the (long-lived) subradiant state $|\psi(t - t_0)\rangle \propto (|e_1,\ g_2\rangle - |g_1,\ e_2\rangle)$. From the latter state, the dimer can undergo a quantum jump into the ground state described by the collective operator $(\sigma_-^1 - \sigma_-^2)$ and emit a photon or, with a smaller probability, into the doubly excited state $|e_1,\ e_2\rangle$ by absorbing the next photon. The dimer in the state $|e_1,\ e_2\rangle$ rapidly (on a timescale $<\gamma^{-1}$) decays into the state $|g_1,\ g_2\rangle$ via two subsequent quantum jumps mediated by the collective operator $\sigma_-^1 + \sigma_-^2$ and accompanied by the emission of two photons: the first jump brings the dimer in the superradiant state $\propto(|g_1,\ e_2\rangle + |e_1,\ g_2\rangle)$ while the second one, after a short delay, into the ground state.

Summing over many such 'quantum trajectories' of the random excitation current leads to the time evolution depicted in figure 3(d), finally settling in the non-equilibrium steady state. The latter state can also be obtained as the time average over a single quantum trajectory (see appendix C). It is therefore not surprising that averaging the oscillatory current over time yields a steady state value that is eight orders of magnitude smaller (compare figures 3(a)–(c) and (d)). However, only in an asymmetric dimer system $(\Delta \neq 0)$ this value is strictly distinct from zero, resulting in a directed excitation flow.

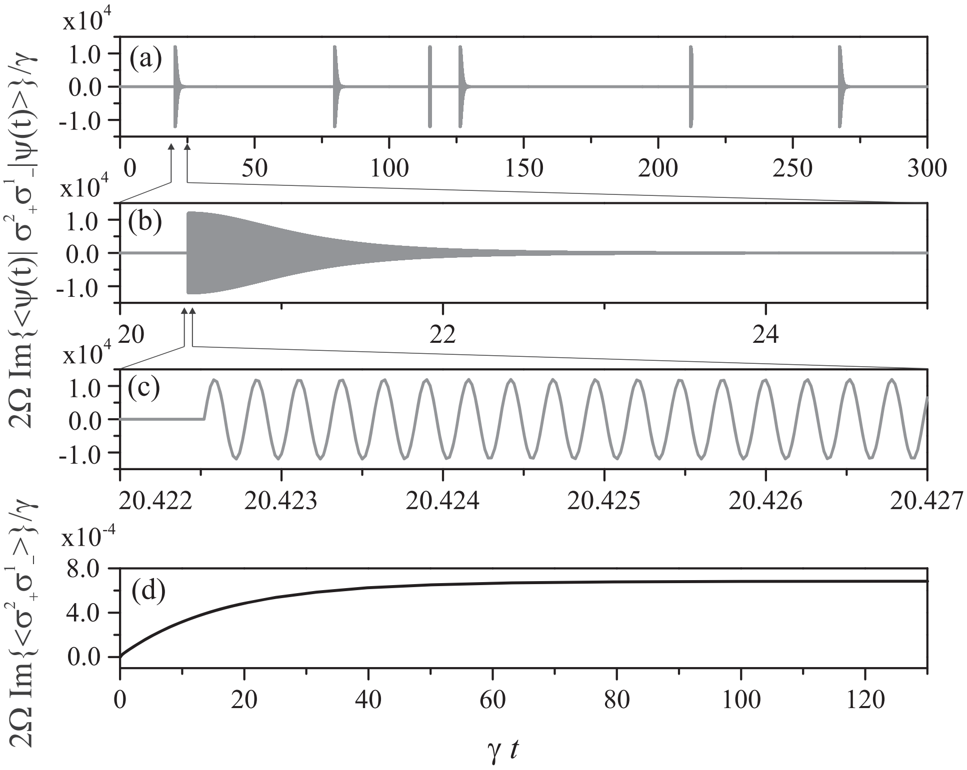

Figure 3. The intermolecular excitation current at $\xi = 0.05$, $\mathrm{f} = 0$, and $\Delta = 50\gamma$ obtained as (a)–(c) quantum mechanical expectation value with respect to the 'quantum trajectory' $|\psi(t)\rangle$, where (a) displays the first six coherent transients of the current initiated (interrupted) by photon absorption (emission) events, (b) zooms in the first coherent transient which tends to a finite value (indiscernible in the plot) at $\gamma(t - t_0) \gtrsim 10\gamma^{-1}$ before the next jump occurs, and (c) zooms in a sequence of coherent oscillations of the current following the first thermal photon absorption. The initially (right after photon absorption) positive current indicates that the photon has been absorbed by molecule 2. (d) Ensemble average over random realizations of $|\psi(t)\rangle$ yields the intermolecular excitation current $2\Omega\,\mathrm{Im}\{\langle\sigma_+^2\sigma_-^1\rangle\}/\gamma$. Note the different scale of the $y-$ axis in (d) as compared to (a)–(c).

4. Conclusion

We have studied the dynamics of the electronic coherence of a toy 'molecular aggregate' composed of two closely located two-level atoms coupled to a vacuum reservoir and excited by an incoherent field. This model accounts of the single-photon excitation process which is crucial [42–44] for understanding the dynamics of the energy transfer in light-harvesting systems. We have shown that, following the photoabsorption by either of the molecules, the transient behavior of this quantity exhibits coherent oscillations which are indicative of the excitation exchange between the dimer's constituents. The amplitude, frequency and decay rate of these oscillations are defined by the inter-molecular dipole–dipole interaction strength and by the local relaxation rates of the individual molecular sites' excitations. Furthermore, we have established the emergence of *stationary* coherence in the non-equilibrium steady state of the aggregate, giving rise to a stationary current, as a consequence of dipole interaction-induced collective decay processes which prevail at small inter-molecular distances, despite being usually associated with the retarded limit. When neglected in a non-retarded theoretical description of the system [22], the incoherent excitation instantaneously creates an incoherent mixture of eigenstates, and steady state coherence is absent. Thus, in contrast to the results of [9], our results establish a realistic scenario where intermolecular electronic steady state coherence can be triggered by the absorption of photons coming from an incoherent source, mediating transient population oscillations which relax into a coherent and directed flux of excitations in the steady state. In the future, it will be interesting to look at the interplay between light-mediated coherence and the vibrational degrees of freedom, which could give rise to unexpected effects.

Finally, the emergence of the excitation current studied here is somewhat akin to the directed flow of electrons [45], phonons [46] or atoms [47] in presence of relaxation, but, unlike the latter examples, features a coherent transfer process driven by collective decay. Thus, the predicted effect defines a hitherto ignored potential resource for generating quantum transport.

Acknowledgments

The authors are grateful to Graham Fleming and Greg Scholes for stimulating discussions. AB thanks Dieter Jaksch and Keble College for their generous hospitality in spring 2016. AB and VNS acknowledge support through the EU Collaborative project QuProCS (Grant Agreement 641277). MW would like to thank the German National Academic Foundation for financial support. FS acknowledges financial support of the European Research Council under the European Union's Seventh Framework Programme (FP7/2007-2013)/ERC Grant Agreement No. 319286 Q-MAC. The authors acknowledge support by the state of Baden-Würtemberg through bwHPC.

Appendix A. Eigensystem of the dimer

The first two terms of the master equation (1) correspond to the Hamiltonian of the dimer $H_D = \hbar\sum_{k\neq l=1}^{2}\left(\frac{\Delta}{2}(-1)^{k-1}\sigma_+^k\sigma_-^k + \Omega\sigma_+^k\sigma_-^l\right)$, where the dipole–dipole interaction couples the states $|e_1, g_2\rangle$ and $|g_1, e_2\rangle$ of the non-interacting molecules. The diagonalization of H_D in the latter subspace yields the Dicke eigensystem, with the eigenvalues $\lambda_\pm = \pm\hbar\,(4\Omega^2 + \Delta^2)^{1/2}/2 \equiv \pm\hbar\,\Omega'/2$ and the corresponding eigenvectors,

$$|\psi_+\rangle = (\cos\theta|e_1, g_2\rangle + \sin\theta|g_1, e_2\rangle), \tag{A.1a}$$

$$|\psi_-\rangle = (-\sin\theta|e_1, g_2\rangle + \cos\theta|g_1, e_2\rangle), \tag{A.1b}$$

for $\Omega > 0$, and

$$|\psi_+\rangle = (-\cos\theta|e_1, g_2\rangle + \sin\theta|g_1, e_2\rangle), \tag{A.2a}$$

$$|\psi_-\rangle = (\sin\theta|e_1, g_2\rangle + \cos\theta|g_1, e_2\rangle), \tag{A.2b}$$

for $\Omega < 0$, where $\theta = \arctan(2|\Omega|/\Delta)/2$ and we assume $\Delta > 0$. It is easy to check the two equalities that hold for the states in (A.1) and (A.2):

$$|\psi_-\rangle\langle\psi_+| - |\psi_+\rangle\langle\psi_-| = \begin{cases} \sigma_2^+\sigma_1^- - \sigma_1^+\sigma_2^- & \text{for} \quad \Omega > 0,\\ \sigma_1^+\sigma_2^- - \sigma_2^+\sigma_1^- & \text{for} \quad \Omega < 0. \end{cases} \tag{A.3}$$

By performing the quantum mechanical average and multiplying both sides of equation (A.3) by $2|\Omega|$, we obtain

$$2|\Omega|\ \mathrm{Im}\ \{\langle|\psi_-\rangle\langle\psi_+|\rangle\} = 2|\Omega| \begin{cases} \mathrm{Im}\ \{\langle\sigma_2^+\sigma_1^-\rangle\} & \text{for} \quad \Omega > 0,\\ \mathrm{Im}\ \{\langle\sigma_1^+\sigma_2^-\rangle\} & \text{for} \quad \Omega < 0. \end{cases} \tag{A.4}$$

The first case ($\Omega > 0$) implies that if the current is downhill in the uncoupled basis (i.e. from $|e_1, g_2\rangle$ to $|g_1, e_2\rangle$) it is also downhill in the eigenbasis (i.e. from $|\psi_+\rangle$ to $|\psi_-\rangle$), whereas the second case means that the uphill current (from $|g_1, e_2\rangle$ to $|e_1, g_2\rangle$) in the uncoupled basis nevertheless corresponds to the downhill current in the eigenbasis. In either scenario, the absolute value of the current in the local basis and in the eigenbasis coincide.

Appendix B. Solution of the master equation (1)

The master equation (1) is equivalent to a closed linear system of 15 equations of motion for the expectation values of the (individual and collective) molecular operators. It is convenient to represent these values as elements of a vector $\langle\vec{Q}\rangle$:

$$\begin{aligned} \langle\vec{Q}\rangle = (&\langle\sigma_-^1\rangle, \langle\sigma_+^1\rangle, \langle\sigma_z^1\rangle, \langle\sigma_-^2\rangle, \langle\sigma_+^2\rangle, \langle\sigma_z^2\rangle, \langle\sigma_-^1\sigma_-^2\rangle,\\ &\langle\sigma_-^1\sigma_+^2\rangle, \langle\sigma_-^1\sigma_z^2\rangle, \langle\sigma_+^1\sigma_-^2\rangle, \langle\sigma_+^1\sigma_+^2\rangle, \langle\sigma_+^1\sigma_z^2\rangle,\\ &\langle\sigma_z^1\sigma_-^2\rangle, \langle\sigma_z^1\sigma_+^2\rangle, \langle\sigma_z^1\sigma_z^2\rangle)^T, \end{aligned} \tag{B.1}$$

where $\sigma_z^k = |e_k\rangle\langle e_k| - |g_k\rangle\langle g_k|$, and for an arbitrary operator O, $\langle O\rangle = \mathrm{Tr}(O\varrho)$. There is a unique relation between the expectation values in (B.1) and the density matrix elements. For instance, $\langle\sigma_-^1\rangle = \mathrm{Tr}(|e_1\rangle\langle g_1|\varrho) = \langle g_1|\varrho^1|e_1\rangle$, where $\varrho^1 = \mathrm{Tr}_2(\varrho)$ is the reduced density matrix of molecule 1, which is obtained upon tracing over the states of molecule 2. The resulting system of equations splits into four uncoupled subsystems. For reference, all entries of the vector $\langle\vec{Q}\rangle$ are listed below according to these subsystems:

$$\begin{array}{ll} \text{(i)} & \langle\sigma_-^1\sigma_-^2\rangle,\ \langle\sigma_+^1\sigma_+^2\rangle, \\ \text{(ii)} & \langle\sigma_-^1\rangle,\ \langle\sigma_-^2\rangle,\ \langle\sigma_-^1\sigma_z^2\rangle,\ \langle\sigma_z^1\sigma_-^2\rangle, \\ \text{(iii)} & \langle\sigma_+^1\rangle,\ \langle\sigma_+^2\rangle,\ \langle\sigma_+^1\sigma_z^2\rangle,\ \langle\sigma_z^1\sigma_+^2\rangle, \\ \text{(iv)} & \langle\sigma_z^1\rangle,\ \langle\sigma_z^2\rangle,\ \langle\sigma_+^2\sigma_-^1\rangle,\ \langle\sigma_+^1\sigma_-^2\rangle,\ \langle\sigma_z^1\sigma_z^2\rangle. \end{array} \tag{B.2}$$

The variables that are here relevant for us are contained in group (iv). Indeed, the excitation current can be expressed as a difference between the number of excitations transferred per unit time from molecule 1 to molecule 2, minus the number of excitations that are transferred in the opposite direction, i.e. it is proportional to the two-molecule coherence function

$$\frac{1}{2\mathrm{i}}(\langle\sigma_+^2\sigma_-^1\rangle - \langle\sigma_+^1\sigma_-^2\rangle) = \ \mathrm{Im}\ \{\langle\sigma_+^2\sigma_-^1\rangle\}. \tag{B.3}$$

The latter quantity can be inferred from solutions of the following equation of motion:

$$\dot{\vec{x}} = A\vec{x} + \vec{L}, \tag{B.4}$$

with $\vec{x} = (\langle\sigma_z^1\rangle,\ \langle\sigma_z^2\rangle,\ \langle\sigma_+^2\sigma_-^1\rangle,\ \langle\sigma_+^1\sigma_-^2\rangle,\ \langle\sigma_z^1\sigma_z^2\rangle)^T$,

$$A = \begin{pmatrix} -\kappa_1 & 0 & -2T^* & -2T & 0 \\ 0 & -\kappa_2 & -2T & -2T^* & 0 \\ \frac{T}{2} & \frac{T^*}{2} & -\frac{\kappa_1+\kappa_2}{2} - \mathrm{i}\Delta & 0 & \Gamma \\ \frac{T^*}{2} & \frac{T}{2} & 0 & -\frac{\kappa_1+\kappa_2}{2} + \mathrm{i}\Delta & \Gamma \\ -2\gamma_2 & -2\gamma_1 & 4\Gamma & 4\Gamma & -\kappa_1-\kappa_2 \end{pmatrix}, \tag{B.5}$$

$$\vec{L} = (-2\gamma_1,\ -2\gamma_2,\ 0{,}0{,}0)^T, \tag{B.6}$$

where $\kappa_i = 2\gamma_i\{1 + 2N(\omega_0)\}$, and $T = \Gamma + \mathrm{i}\Omega$, with $\Gamma \equiv \Gamma(\xi)$, $\Omega \equiv \Omega(\xi)$ given by (2*a*) and (2*b*), respectively. We assume that at time $t = 0$ both molecules are in their ground states, hence the vector of initial conditions is

$$\vec{x}(0) = (-1,\ -1{,}0,\ 0{,}1)^T. \tag{B.7}$$

The formal time dependent solution of (B.4) reads

$$\vec{x}(t) = e^{At}\vec{x}(0) + (e^{At} - \mathbb{1})A^{-1}\vec{L}. \tag{B.8}$$

For arbitrary times, the temporal behavior of $\vec{x}(t)$ can be studied numerically and in figure 2 we present exemplary evolutions of the excitation current $2\Omega\,\mathrm{Im}\{x_3(t)\}$. This quantity exhibits monotonic behavior, wherein the current exponentially tends to its stationary value.

Let us now address this limit, where analytical solutions $\vec{x}(\infty) = -A^{-1}\vec{L}$ are readily available.

First, let us consider the steady state solutions for $\Gamma = 0$. In this case, the entries of the vector $\vec{x}(\infty)$ read:

$$\langle\sigma_z^1\rangle = \langle\sigma_z^2\rangle = -\frac{1}{1 + 2N}, \tag{B.9}$$

$$\langle\sigma_+^2\sigma_-^1\rangle = \langle\sigma_+^1\sigma_-^2\rangle = 0, \tag{B.10}$$

$$\langle\sigma_z^1\sigma_z^2\rangle = \langle\sigma_z^1\rangle\langle\sigma_z^2\rangle, \tag{B.11}$$

where $N \equiv N(\omega_0)$. The above solutions indicate equal population distributions of both molecules and the absence of intermolecular electronic coherence.

In contrast, for $\Gamma \neq 0$, we obtain $\langle\sigma_z^1\rangle \neq \langle\sigma_z^2\rangle$, and a non-trivial two-molecule coherence in the two-level system. Below we present the explicit expressions for two quantities: the excitation current, $\mathrm{Im}\ \{\langle\sigma_+^2\sigma_-^1\rangle\}$, and the difference between the excited state populations of the two molecules, $\langle\sigma_+^2\sigma_-^2\rangle - \langle\sigma_+^1\sigma_-^1\rangle = (\langle\sigma_z^2\rangle - \langle\sigma_z^1\rangle)/2$:

$$\mathrm{Im}\ \{\langle\sigma_-^1\sigma_+^2\rangle\} = \frac{2N\Gamma[(1+2N)\gamma_1\gamma_2\Delta + (\gamma_2-\gamma_1)\Gamma\Omega]}{R}, \tag{B.12}$$

$$\langle\sigma_+^2\sigma_-^2\rangle - \langle\sigma_+^1\sigma_-^1\rangle = \frac{2N\Gamma(\gamma_1+\gamma_2)[\Delta\Omega + (\gamma_1-\gamma_2)(1+2N)\Gamma]}{R}, \tag{B.13}$$

with

$$\begin{aligned} R = {} & 2(1+2N)(\gamma_2-\gamma_1)\Delta\Gamma\Omega + \Gamma^2[(1 + 2N)^2 \\ & \times \{2N(\gamma_1-\gamma_2)^2 - (\gamma_1+\gamma_2)^2\} - 4\Omega^2] \\ & + (1 + 2N)^3[\gamma_1\gamma_2\{(1 + 2N)^2(\gamma_1+\gamma_2)^2 + \Delta^2\} \\ & + (\gamma_1+\gamma_2)^2\Omega^2]. \end{aligned} \tag{B.14}$$

Direct inspection of (B.12) and (B.13), for $\gamma = \gamma_1 = \gamma_2$, yields the energy balance relation (5).

Appendix C. Monte-Carlo simulation of the stochastic current

As shown in [40, 48], a density operator $\varrho(t)$ obeying a Markov master equation with a relaxation in Lindblad form can be unraveled into an ensemble of stochastic wavefunctions (quantum trajectories) $|\psi(t)\rangle$, such that averaging over possible outcomes at time t yields the density operator, i.e.

$$\overline{|\psi(t)\rangle\langle\psi(t)|} = \varrho(t). \tag{C.1}$$

Quantum trajectories corresponding to master equations with a unique steady state possess the property of ergodicity [49]. Therefore, when one deals with a steady state density matrix, it is more convenient to use the time average over a single trajectory instead of the ensemble average [50].

The master equation (1) is not given in Lindblad form, but can be brought into it by a unitary transformation applied to the second line of (1). Then we obtain

$$\dot{\varrho} = -(\mathrm{i}/\hbar)[H_D, \varrho] + \mathscr{L}(\varrho), \tag{C.2}$$

where H_D is given in appendix A. Thereby, equation (1) turns into the Lindblad equation and

$$\mathscr{L}(\varrho) = \sum_k^4 \left(A_k \varrho A_k^\dagger - \frac{1}{2}\{A_k^\dagger A_k, \varrho\}\right), \tag{C.3}$$

with $A_1 = \sqrt{2\gamma N}\sigma_+^1$, $A_2 = \sqrt{2\gamma N}\sigma_+^2$, $A_3 = \sqrt{\gamma(1+N) - \Gamma}(\sigma_-^2 - \sigma_-^1)$, $A_4 = \sqrt{\gamma(1+N) + \Gamma}(\sigma_-^2 + \sigma_-^1)$. We note that the contributions due to the Lindblad operators A_1, A_2, are A_3 are much smaller than the one due to A_4 (since $N = 0.01$ and we consider the intermolecular distances such that $\Gamma \approx \gamma$).

First, we define the effective non-Hermitian Hamiltonian

$$H_{\mathrm{eff}} = H_D - (\mathrm{i}\hbar/2)\sum_k A_k^\dagger A_k. \tag{C.4}$$

Using (C.2), (C.4), we perform a stochastic unraveling as described in [41]. We assume that the molecular aggregate is initially in its ground state, that is, $|\psi(0)\rangle = |g_1, g_2\rangle$, and divide the time axis into infinitesimal intervals δt which should be much shorter than the shortest characteristic system time scale defined by Ω. To generate the exemplary trajectory of the stochastic current in figure 3, we fix $\delta t = 2.0 \times 10^{-5}\gamma^{-1}$ and $\Omega^{-1} \approx 8.4 \times 10^{-5}\gamma^{-1}$. At each time step, we calculate the probability

$$\delta p = \mathrm{i}\delta t\langle\psi(t)|H_{\mathrm{eff}} - H_{\mathrm{eff}}^\dagger|\psi(t)\rangle/\hbar, \tag{C.5}$$

that the system evolves continuously, and update the quantum state as follows: we compared δp with a random number ϵ uniformly distributed on the interval [0,1]. If $\delta p < \epsilon$, then $|\psi(t+\delta t)\rangle$ is given by

$$|\psi(t+\delta t)\rangle = (1 - (\mathrm{i}/\hbar H_{\mathrm{eff}})\delta t)|\psi(t)\rangle/(1-\delta p)^{1/2}. \tag{C.6}$$

At this stage, the state continuously evolves, undergoing coherent oscillations at the frequency Ω' given by the eigenvalues of H_D (see above). If $\delta p \geqslant \epsilon$, then a 'quantum jump' occurs, whereby the state changes according to

$$|\psi(t+\delta t)\rangle = A_m|\psi(t)\rangle/(\delta p_m/\delta t)^{1/2}, \quad (m = 1, \ldots, 4) \tag{C.7}$$

with

$$\delta p_m = \delta t\langle\psi(t)|A_m^\dagger A_m|\psi(t)\rangle, \quad \sum_m \delta p_m = \delta p. \tag{C.8}$$

It follows from the definitions of the jump operators A_m that if the aggregate is in its ground state, a photoabsorption can be mediated by either A_1 or A_2, with the equal probability of 1/2. Once a photon is absorbed at a random time $t_0 > 0$, the probability p_4 of the photoemission associated with the operator A_4 is much larger than p_3, associated with A_3 (see above). Furthermore, because $N \ll 1$, the probability of double excitation is very low. However, if the next quantum jump does not occur until times $t - t_0 \gtrsim 10\gamma^{-1}$, the dimer is effectively driven into the antisymmetric state $\propto|e_1, g_2\rangle - |g_1, e_2\rangle$, wherefrom it can undergo a jump either into the ground state mediated by the operator A_3, with the probability of $\approx 1/2$, or into the doubly excited state mediated by the operators A_1 or A_2 (each event with approximately equal probability of $\approx 1/4$).

To show why the dimer's state conditioned by the absence of a quantum jump following a photoabsorption becomes, at long times, the antisymmetic state, we turn to the non-unitary evolution operator generated by H_{eff}. This operator reads (in the basis $\{|g_1, g_2\rangle, |e_1, g_2\rangle, |g_1, e_2\rangle, |e_1, e_2\rangle\}$):

$$\mathrm{e}^{-\frac{\mathrm{i}H_{\mathrm{eff}}t}{\hbar}} = \mathrm{e}^{-(1+2N)\gamma t}\begin{pmatrix} \mathrm{e}^{\gamma t} & 0 & 0 & 0 \\ 0 & \cosh\left(\frac{\Omega'' t}{2}\right) - \frac{\mathrm{i}\Delta \sinh\left(\frac{\Omega'' t}{2}\right)}{\Omega''}) & -\frac{2(\Gamma + \mathrm{i}\Omega)\sinh\left(\frac{\Omega'' t}{2}\right)}{\Omega''} & 0 \\ 0 & -\frac{2(\Gamma + \mathrm{i}\Omega)\sinh\left(\frac{\Omega'' t}{2}\right)}{\Omega''} & \cosh\left(\frac{\Omega'' t}{2}\right) + \frac{\mathrm{i}\Delta \sinh\left(\frac{\Omega'' t}{2}\right)}{\Omega''}) & 0 \\ 0 & 0 & 0 & 1 \end{pmatrix}, \tag{C.9}$$

where $\Omega'' = \sqrt{4\Gamma^2 - \Delta^2 - 4\Omega^2 + 8\mathrm{i}\Gamma\Omega}$ is a complex frequency with $\mathrm{Im}\ \Omega'' \approx \Omega'$ (see appendix A) and $0 < \ \mathrm{Re}\ \Omega'' < 2\gamma$. Let us assume that at $t_0 > 0$ the dimer jumps into state $|e_1,\ g_2\rangle$ via photoabsorption by molecule 1. At short times $(t - t_0) \ll \gamma^{-1}$, $\exp(-\mathrm{i}H_{\mathrm{eff}}(t - t_0)/\hbar) \approx \exp(-\mathrm{i}H_D(t - t_0)/\hbar)$, such that H_{eff} generates oscillations at the frequency Ω' of the probability amplitudes associated with the states $|e_1,\ g_2\rangle$ and $|g_1,\ e_2\rangle$ (coherent excitation exchange between the molecules). At long times $(t - t_0) \gtrsim 10\gamma^{-1}$, the dominant contribution to the relaxation part of H_{eff} is given by the operator $-(\mathrm{i}\hbar/2)A_4^\dagger A_4 \propto (\sigma_+^1 + \sigma_+^2)(\sigma_-^1 + \sigma_-^2)$. Consequently, the symmetric superpositions $|e_1,\ g_2\rangle + |g_1,\ e_2\rangle$, also known as superradiant states [11, 31], decay faster than the antisymmetric (subradiant) states $|e_1,\ g_2\rangle - |g_1,\ e_2\rangle$ and the conditioned state is given by

$$|\psi(t - t_0)\rangle_c = \exp[\{\Omega''/2 - (1 + 2N)\gamma\}(t - t_0)](a|e_1,\ g_2\rangle + b|g_1,\ e_2\rangle), \tag{C.10}$$

where $a = 1/2 - \mathrm{i}\Delta/(2\Omega'')$ and $b = -(\Gamma + \mathrm{i}\Omega)/\Omega'' \approx -a$. Hence, $|\psi(t - t_0)\rangle_c \propto |e_1,\ g_2\rangle - |g_1,\ e_2\rangle$.

Given a normalized state $|\psi(t)\rangle$, we determine the stochastic excitation current by

$$I_{\mathrm{stoch}}(t) = 2\Omega\ \mathrm{Im}\ \{\langle\psi(t)|\sigma_+^2\sigma_-^1|\psi(t)\rangle\}. \tag{C.11}$$

In particular, normalizing the state (C.10), we obtain that the corresponding conditioned excitation current is time-independent:

$$I_c = \frac{2\Omega\ \mathrm{Im}\ (ab^*)}{|a|^2 + |b|^2}, \tag{C.12}$$

and, for the parameters chosen in figure 3, $I_c \approx 0.0021\gamma^{-1}$.

By virtue of (C.1), the average over the ensemble of random realizations of $|\psi(t)\rangle$ in (C.11) yields the average excitation current as given by (4). On the other hand, the average steady state current can be obtained by the time average over a single quantum trajectory

$$\bar{I}_{\mathrm{stoch}}(\infty) = \lim_{T\to\infty}\frac{1}{T}\int_0^T \mathrm{d}t\ \ I_{\mathrm{stoch}}(t). \tag{C.13}$$

References

[1] Scholes G D, Fleming G R, Olaya-Castro A and van Grondelle R 2011 *Nat. Chem.* **3** 763
[2] Blanckenship R E 2002 *Molecular Mechanisms of Photosynthesis* (Oxford: Oxford University Press)
[3] Scholes G D *et al* 2017 *Nature* **543** 647
[4] Duan H G, Prokhorenko V I, Cogdell R J, Ashraf K, Stevens A L, Thorwart M and Miller R J D 2017 *Proc. Natl Acad. Sci. USA* **114** 8493
[5] Brixner T, Stenger J, Vaswani H M, Cho M, Blankenship R E and Fleming G R 2005 *Nature* **434** 625
[6] Engel G S, Calhoun T R, Read E L, Ahn T K, Mancal T, Cheng Y C, Blankenship R E and Fleming G R 2007 *Nature* **446** 782
[7] Andrea Rozzi C *et al* 2013 *Nat. Commun.* **4** 1602
[8] Falke S M *et al* 2014 *Science* **344** 1001
[9] Brumer P and Shapiro M 2012 *Proc. Natl Acad. Sci. USA* **109** 19575
[10] Mukamel S 1999 *Principles of Nonlinear Optical Spectroscopy* (New York: Oxford University Press)
[11] Mandel L and Wolf E 1995 *Optical Coherence and Quantum Optics* (Cambridge: Cambridge University Press)
[12] Christensson N, Kauffmann H F, Pullerits T and Mančal T 2012 *J. Phys. Chem.* B **116** 7449
[13] Pachón L A and Brumer P 2013 *Phys. Rev.* A **87** 022106
[14] Mančal T and Valkunas L 2010 *New J. Phys.* **12** 065044
[15] Cheng Y C and Fleming G R 2009 *Annu. Rev. Phys. Chem.* **60** 241
[16] Ishizaki A and Fleming G R 2012 *Annu Rev. Condens. Matter Phys.* **3** 333
[17] Manzano D, Tiersch M, Asadian A and Briegel H J 2012 *Phys. Rev.* E **86** 061118
[18] Dorfman K E, Voronine D V, Mukamel S and Scully M O 2013 *Proc. Natl Acad. Sci. USA* **110** 2746
[19] Strümpfer J, Şener M and Schulten K 2012 *J. Phys. Chem. Lett.* **3** 536
[20] Dostál J, Pšenčík J and Zigmantas D 2016 *Nat. Chem.* **8** 705
[21] Collini E, Wong C Y, Wilk K E, Curmi P M G, Brumer P and Scholes G D 2010 *Nature* **463** 644
[22] May V and Kühn O 2004 *Charge and Energy Transfer Dynamics in Molecular Systems* (Weinheim: Wiley-VCH)
[23] Renger T, May V and Kühn O 2001 *Phys. Rep.* **343** 137
[24] Loudon R 2004 *The Quantum Theory of Light* 3rd edn (Oxford: Oxford University Press)
[25] Scully M O and Zubairy M S 1997 *Quantum Optics* (Cambridge: Cambridge University Press)
[26] Agarwal G S 1974 *Quantum Statistical Theories of Spontaneous Emission and their Relation to other Approaches* (Berlin: Springer)
[27] Andrews D L and Sherborne B S 1987 *J. Chem. Phys.* **86** 4011
[28] Salam A 2010 *Molecular Quantum Electrodynamics* (New York: Wiley)
[29] Frost J E and Jones G A 2014 *New J. Phys.* **16** 113067

[30] Gross M and Haroche S 1982 *Phys. Rep.* **93** 301
[31] Ficek Z and Tanaś R 2002 *Phys. Rep.* **372** 369
[32] Lehmberg R H 1970 *Phys. Rev.* A **2** 883
[33] Milder M, Brüggemann B, van Grondelle R and Herek J L 2010 *Photosynth. Res.* **104** 257
[34] Scholak T, de Melo F, Wellens T, Mintert F and Buchleitner A 2011 *Phys. Rev.* E **83** 021912
[35] Olšina J, Dijkstra A G, Wang C and Cao J 2014 arXiv:1408.5385
[36] Tscherbul T V and Brumer P 2014 *Phys. Rev. Lett.* **113** 113601
[37] Tscherbul T V and Brumer P 2018 *J. Chem. Phys.* **148** 124114
[38] Cohen-Tannoudji C, Dupont-Roc J and Grynberg G 1992 *Atom-Photon Interactions* (New York: Wiley)
[39] Shatokhin V N and Kilin S Y 2002 *Opt. Commun.* **210** 291
[40] Carmichael H J 1993 *An Open Systems Approach to Quantum Optics* (Berlin: Springer)
[41] Mølmer K, Castin Y and Dalibard J 1993 *J. Opt. Soc. Am.* B **10** 524
[42] Brumer P 2018 *J. Phys. Chem. Lett.* **9** 2946
[43] Pachón L A, Botero J D and Brumer P 2017 *J. Phys. B: At. Mol. Opt. Phys.* **50** 184003
[44] Chan H C H, Gamel O E, Fleming G R and Whaley K B 2018 *J. Phys. B: At. Mol. Opt. Phys.* **51** 054002
[45] Anderson P W 1992 *Concepts in Solids: Lectured on the Theory of Solids* (New York: Addison-Wesley)
[46] Kilin S Y, Maevskaya T M, Nizovtsev A P, Shatokhin V N, Berman P R, von Borczyskowski C, Wrachtrup J and Fleury L 1998 *Phys. Rev.* A **57** 1400
[47] Ponomarev A V, Madroñero J, Kolovsky A R and Buchleitner A 2006 *Phys. Rev. Lett.* **96** 050404
[48] Dalibard J, Castin Y and Mølmer K 1992 *Phys. Rev. Lett.* **68** 580
[49] Kümmerer B and Maassen H 2003 *J. Phys. A: Math. Gen.* **36** 2155
[50] Gardiner C W and Zoller P 2004 *Quantum Noise* 3rd edn (Berlin: Springer)